Bull Volcanol (2012) 74:2435–2448
DOI 10.1007/s00445-012-0673-2

RESEARCH ARTICLE

Diffuse volcanic degassing and thermal energy release from Hengill volcanic system, Iceland

Pedro A. Hernández · Nemesio M. Pérez · Thráinn Fridriksson · Jolie Egbert · Evgenia Ilyinskaya · Andri Thárhallsson · Gretar Ívarsson · Gestur Gíslason · Ingvi Gunnarsson · Birgir Jónsson · Eleazar Padrón · Gladys Melián · Toshiya Mori · Kenji Notsu

Received: 25 January 2012 / Accepted: 21 October 2012 / Published online: 9 November 2012

Abstract We report the first detailed study of spatial variations on the diffuse emission of carbon dioxide (CO_2) and hydrogen sulfide (H_2S) from Hengill volcanic system, Iceland. Soil CO_2 and H_2S efflux measurements were performed at 752 sampling sites and ranged from nondetectable to 17,666 and 722 $g\,m^{-2}\,day^{-1}$, respectively. The soil temperature was measured at each sampling site and used to evaluate the heat flow. The chemical composition of soil gases sampled at selected sampling sites during this study shows they result from a mixing process between deep volcanic/hydrothermal component and air. Most of the diffuse CO_2 degassing is observed close to areas where active thermal manifestations occur, northeast flank of the Hengill central volcano close to the Nesjavellir power plant, suggesting a diffuse degassing structure with a SSW–NNE trend, overlapping main fissure zone and indicating a structural control of the degassing process. On the other hand, H_2S efflux values are in general very low or negligible along the study area, except those observed at the northeast flank of the Hengill central volcano, where anomalously high CO_2 efflux and soil temperatures were also measured. The total diffuse CO_2 emission estimated for this volcanic system was about 1,526±160 $t\,day^{-1}$ of which 453 $t\,day^{-1}$ (29.7 %) are of volcanic/hydrothermal origin. To calculate the steam discharge associated with the volcanic/hydrothermal CO_2 output, we used the average H_2O/CO_2 mass ratio from 12

Editorial responsibility: P. Delmelle

P. A. Hernández (✉) · N. M. Pérez · E. Padrón · G. Melián
Environmental Research Division,
Instituto Tecnológico y de Energías Renovables (ITER),
38611 Granadilla de Abona, Santa Cruz de Tenerife, Spain
e-mail: phdez@iter.es

P. A. Hernández · N. M. Pérez · E. Padrón · G. Melián
Instituto Volcanológico de Canarias (INVOLCAN),
Antiguo Hotel Taoro, Parque Taoro, 22,
38400 Puerto de La Cruz, Tenerife, Spain

T. Fridriksson · J. Egbert · E. Ilyinskaya · A. Thárhallsson
Iceland GeoSurvey (ISOR),
Grensásvegi 9,
108 Reykjavík, Iceland

G. Ívarsson · G. Gíslason · I. Gunnarsson
Reykjavik Energy (Orkuveita Reykjavíkur),
Bæjarhálsi 1,
110 Reykjavík, Iceland

B. Jónsson
Civil and Environmental Engineering Department,
University of Iceland,
Hjarðarhagi 2-6,
107 Reykjavík, Iceland

T. Mori · K. Notsu
Geochemical Research Center, Graduate School of Science,
The University of Tokyo,
Hongo, Bunkyo-Ku,
113-0033 Tokyo, Japan

Present Address:
J. Egbert
Helmholtz Centre Potsdam, GFZ German Research Centre
for Geosciences,
Telegrafenberg,
14473 Potsdam, Germany

fumarole samples equal to 88.6 (range, 9.4–240.2) as a representative value of the H_2O/CO_2 mass ratios for Hengill fumarole steam. The resulting estimate of the steam flow associated with the gas flux is equal to 40,154 $t day^{-1}$. The condensation of this steam results in thermal energy release for Helgill volcanic system of $1.07 \times 10^{14} J day^{-1}$ or to a total heat flow of 1,237 MW_t.

Keywords Diffuse CO_2 emission · Diffuse H_2S emission · Heat flux · Hengill volcano

Introduction

During repose periods, volcanoes can release large amounts of gases through visible (fumaroles, solfataras, and plumes) and nonvisible (diffuse degassing) emanations. Degassing from magma and hydrothermal aquifers creates gas anomalies at the surface environment as a result of advective and diffusive gas transport mechanisms. The surface manifestations of degassing and volatile emanations are usually controlled by the volcano-tectonics and hydrology of the volcanic system in which permeable structures direct the gases to the surface. Among investigations of diffuse degassing phenomena, CO_2 efflux studies of volcanoes (Hernández et al. 2001a, b, 2003, 2006; Rogie et al. 2001; Brombach et al. 2001; Granieri et al. 2006; Lewicki et al. 2007; Carapezza et al. 2011) have played an important role because of the special characteristics of CO_2: it is the major gas species after water vapor in both volcanic fluids and magmas and it is an effective tracer of subsurface magma degassing because of its low solubility in silicate melts at low to moderate pressures, favoring its early exsolution (Gerlach and Graeber 1985). Most of the diffuse CO_2 degassing studies carried out at volcanoes have involved mapping the volcanic structures to better understand the processes occurring at depth and to monitor the spatial distribution, magnitude, and temporal evolution of the surface anomalies (Baubron et al. 1990; Allard et al. 1991; Chiodini et al. 1996, 1998, 2001; Frondini et al. 2004; Gerlach et al. 2001; Hernández et al. 1998, 2001a, 2003, 2006; Notsu et al. 2005; Padrón et al. 2007, 2008; Pérez et al. 2004, 2006; Salazar et al. 2001, 2004). Because the rate of diffuse CO_2 emission can increase by as much as two or three orders of magnitude before a volcanic eruption (Hernández et al. 2001a; Carapezza et al. 2004), it is very important to estimate the total CO_2 output in order to investigate the magma volume within a volcano's magma reservoir and its hydrothermal system and to infer any changes occurring in a volcano's magma reservoir (Gerlach et al. 2001; Toutain et al. 1992; Salazar et al. 2001).

In contrast to CO_2 investigations, there are very few studies on diffuse H_2S at volcanic areas because the gas is much harder to detect. An important characteristic of H_2S is that it is the dominant sulfur species at hydrothermal conditions and in low-temperature fumaroles and solfataras, where discharges arise from deep hydrothermal systems (Giggenbach 1980), in contrast to SO_2, which is the dominant sulfur species in high-temperature volcanic gas emissions. As a result, studies on diffuse H_2S emissions from the soil in natural degassing areas are rare and relatively recent (Salazar et al. 2005; Pérez et al. 2007; Voltaggio and Spadoni 2009). At Teide volcano (Tenerife, Spain), Salazar et al. (2005) measured CO_2 and H_2S effluxes on the flank of the summit cone, showing close spatial and temporal variations that provided useful information regarding the state of the volcanic system. Voltaggio and Spadoni (2009) studied the diffuse H_2S emissions at the Zolforata di Pomezia degassing area (Alban Hills, Central Italy), estimating a total atmospheric H_2S flux of about 1,208 $kg day^{-1}$.

Another issue that has received increasing attention in recent years is the relationship between heat flow and the degassing process (Chiodini et al. 2001, 2007). This type of geochemical surveillance aims to detect changes in the energy balance of the volcanic system under observation, particularly an increase in heat flow from the magma body. This is based on the relatively high thermal energy outputs estimated for many volcanic–geothermal systems (Chiodini et al. 2001, 2007; Fridriksson et al. 2006; Frondini et al. 2009) and their potentially high variability in energy output as a result of magmatic and tectonic processes.

The main objectives of this work are to study the diffuse CO_2 and H_2S emissions from the Hengill volcano and to estimate the total CO_2 and H_2S output to the atmosphere by this volcanic system. We also estimate the associated thermal energy flux of the diffuse degassing phenomena and compare this thermal energy with heat flow estimates based on soil temperature measurements.

Present Address:
G. Gíslason
Reykjavik Geothermal,
Sudurlandsbraut 18,
108 Reykjavík, Iceland

Present Address:
E. Ilyinskaya
Icelandic Meteorological Office,
Bustadavegi 7-9,
150 Reykjavík, Iceland

Present Address:
K. Notsu
Center for Integrated Research and Education of Natural Hazards (CIREN), Shizuoka University,
Ohya 836, Suruga-ku,
Shizuoka 422-8529, Japan

Geological setting

The Hengill volcanic system lies on the plate boundary between the North American and the European crustal plates. These plates are diverging at a relative motion of 2 cm/year. Three volcanic eruptions are known to have occurred in the Hengill volcanic system over the last 11,000 years, the most recent eruption having taken place 2,000 years ago (Ingólfsson et al. 2008). The last eruption in the vicinity occurred in the year 1000 on a fissure west of Hengill, forming the Svínafellsbruni lava field.

The Hengill volcanic system (Fig. 1) is located in the eastern part of the Reykjanes peninsula at an unstable ridge–ridge–transform triple junction where the Reykjanes Volcanic Zone, the West Volcanic Zone, and the South Iceland Seismic Zone converge (Foulger 1988; Tryggvason et al. 2002). This rift zone is also highly permeable and numerous fumaroles and hot springs are found on surface. Regarding the tectonic situation, it is a zone of high seismic activity (Vogfjörd et al. 2005). The last rifting event was in 1789, with intrusive volcanism, i.e., dyke injection (Foulger 1995; Sæmundsson 2006). The 60- to 80-km long, NNE (25°) striking fissure system is associated with a graben structure continuing to Lake Thingvallavatn in the North as Thingvellir Graben (Tryggvason et al. 2002; Friese et al. 2005). The volcanic system consists of the Hengill central volcano (803 m asl) and other small shield volcanoes, crater rows, eruptive fissure vents, and dissecting normal faults. It is one of Iceland's largest high-temperature geothermal areas with two active geothermal power plants: Nesjavellir and Hellisheidi.

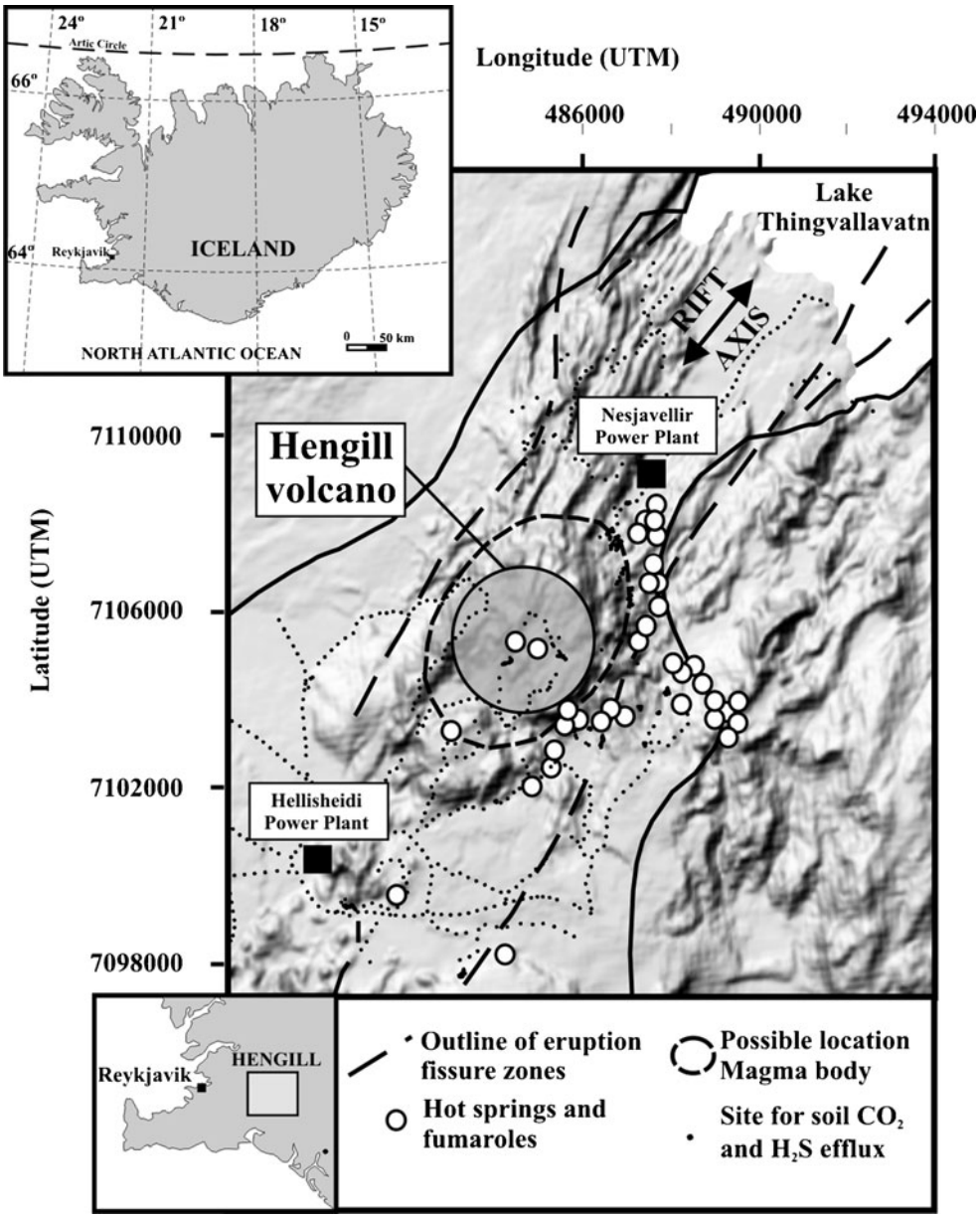

Fig. 1 Map of Iceland showing the location of the Hengill volcanic system. Major faults are shown by *tagged lines* (modified from Bodvarsson et al. 1990). *Black dots* soil CO_2 and H_2S efflux and temperature measurements, *open big circles* hot springs and fumaroles

Observed tectonic and volcanological features indicate shallow, fractionating magma chambers. Beneath the northeastern flank of the Hengill central volcano, an isolated low-velocity body with an estimated partial melt of 7 % was detected in a depth of 2 to 4 km (Foulger and Toomey 1989; Foulger and Arnott 1993).

The Hengill volcanic system is currently active while its predecessor, the Hveragerdi system, is now extinct in terms of volcanic activity but still very active seismically and hosts a high-temperature geothermal reservoir. The area around Hengill volcano was characterized between 1994 and 2000 by a tectonic event consisting of approximately 100,000 microearthquakes, most of them located at 5±3 km depth and grouping on lines striking either E–W or N–S, but surprisingly not to the NNE as seen in surface geology (Árnason and Magnússon 2001; Björnsson et al. 2003). Jousset et al. (2011) integrated velocity models with a resistivity model obtained from transient electromagnetic soundings (TES) and magnetotelluric inversion (Árnason et al. 2010) and identified a low resistivity/high V_P/V_S ratio area at 2.5–4 km depth similar to the earthquake hypocenters and possibly extending deeper. They interpreted this body as the heat source of the Hengill volcanic complex. Above this body, where most seismicity is observed, hot, superheated (possibly supercritical) fluids would upflow in structural features like fault intersections related to the Hengill triple junction.

The vast geothermal systems of the Hengill volcano in SW Iceland are important resources for electrical and heating needs for the city of Reykjavik and surrounding areas (Björnsson et al. 2003; Franzson et al. 2005). For these reasons, extensive geological, geophysical, and geochemical surveys have been carried out in the Hengill area in conjunction with the Nesjavellir and Hellisheidi drilling activities (Björnsson et al. 1986, 2003; Franzson et al. 2005).

Origin of the gas emitted at Hengill volcano

Hengill volcano is characterized by the existence of many fumarole fields, mud pools, and steaming ground. The temperatures of the fumarole steam at Hengill correspond to the boiling point of water at the Hengill elevation (~100 °C) and show a typical hydrothermal composition (Table 1; this study), with H_2O as a major constituent (meteoric origin), followed by CO_2, H_2S, H_2, N_2, CH_4, and He, while CO and acid gases SO_2, HCl, and HF are practically absent (this study; Marty et al. 1991). These authors computed equilibrium temperatures by the geoindicators proposed by Arnórsson and Gunnlaugsson (1985) and observed that the highest temperatures corresponded to wells and fumaroles along the rift axis, in the range 250–300 °C. These temperature estimates are confirmed by the H_2–Ar geoindicator (Chiodini et al. 1998). The whole Hengill volcanic system is characterized by a source having a mean R/R_A of 14.4±1.6 (Marty et al. 1991). They observed that these values were higher than the normal mid-ocean ridge He range of 8±1 and suggested hot-spot helium for Hengill. A clear decrease with distance of the highest chemical temperatures and helium contents from the main axis of the rift was also observed. The mantle beneath the Hengill volcanic system appears to be the direct source of volatiles and gases at the surface environment.

Materials and methods

During August of 2006, a soil CO_2 and H_2S efflux and soil temperature survey was carried out at Hengill volcanic field, Iceland. A total of 752 measurements covered an area of about 168 km^2 and focused mainly on the surface geothermal areas of Nesjavellir geothermal area. Coordinates of the sampling sites were always recorded with portable global positioning systems. Figure 1 shows the sampling sites distribution and the main geothermal surface manifestations at the studied area.

Soil CO_2 and H_2S efflux

Soil CO_2 and H_2S efflux measurement sites were selected to cover most of the Hengill volcanic zone after considering accessibility and main volcano-structural features (Fig. 1). Most of soil gas measurements were done along access roads and hiking trails and around active surface geothermal manifestations. The measurement density was higher around the surface manifestations where the gas flux values were typically higher than elsewhere. The reason for a higher measurement density was to constrain the areal extent of the anomalies.

Measurements of soil CO_2 and H_2S efflux were performed in situ by means of three gas flux meters based on the accumulation chamber method (Parkinson 1981) of two different types: (1) We used two classical West Systems portable CO_2 flux meters equipped with a nondispersive infrared CO_2 analyzer LICOR-800 system composed of a double beam infrared carbon dioxide sensor compensated for temperature and atmospheric pressure, with an accuracy of concentration reading of 2 % and a repeatability of ±5 ppm, and an H_2S electrochemical cell, with a full scale range of 20 ppm, a precision of 3 % of reading, and a repeatability of 1.5 % of span with a zero offset of 0.3 % and (2) an improved version of the classical West Systems portable flux meter, where the carbon dioxide detector is a Vaisala GP343 (see Padrón et al. 2008), allowing CO_2 flux measurements in the range 1–30,000 $g\,m^{-2}day^{-1}$. The latter instrument was not equipped with an H_2S sensor. The gas

Table 1 Chemical composition in volume percent of fumarolic samples collected at the Hengill volcanic system

Fumarole gas sample	Sampling date	H_2	N_2	CH_4	O_2+Ar	H_2S	CO_2	H_2O/CO_2 (weight ratio)
Skíðaskáli	27/06/2007	41.4	308.2	n.m.	7.4	63.4	643.3	34.6
Sleggjubeinsdalur	16/08/2007	44.7	53.5	3.69	4.7	93.1	1,129.9	19.6
Þrymheimar	12/07/2007	4.3	38.0	0.27	0.9	15. 5	273.5	82.6
Innstidalur	12/07/2007	97.1	42.6	9.17	1.7	54.5	2,303.3	9.4
Fremstidalur	12/06/2007	1.4	2.8	0.00	0.2	0.8	133.7	169.5
Hveragerði	12/07/2007	3.7	2.3	0.09	0.1	4.7	94.5	240.2
Reykjadalur	09/07/2008	3.1	6.0	0.03	1.1	5.4	171.9	131.8
Ölkelduháls	27/06/2007	7.3	7.3	0.00	0.6	20.9	406.9	55.4
Ölkelduháls	23/05/2007	1.4	3.7	0.00	0.3	13.1	197.1	114.8
Sandklettar	25/06/2008	25.9	23.0	0.28	4.4	25.3	696.3	32.2
Köldulaugagil	18/06/2008	25.4	11.7	1.26	1.1	25.3	266.3	84.8
Nesjalaugagil	02/06/2008	48.0	18.1	0.03	3.4	47.6	288.6	78.2

The gas concentrations are expressed as millimoles per kilogram

n.m. not measured

flux meters were interfaced to a handheld computer running data acquisition software.

Fumarolic gas sampling

Fumarolic samples were collected between May 2007 and July 2008 at different fumarolic fields of Nesjavellir and Hellisheidi (Table 1), both belonging to the Hengill volcanic system. The gas emissions consisted of fluids discharged at about 90–100 °C, namely, the boiling point of water at the altitude of the fumarolic field. The sampling technique of fumarolic gas was performed following the method described by Arnórsson et al. (2006). CO_2 and H_2S were determined titrimetrically in a solution of a strong alkali (NaOH or KOH), CO_2 by an alkalinity titration with HCl, and H_2S by either iodometry or with mercuric acetate using dithizone as an indicator. Gases that are not absorbed by the strong alkali (N_2, H_2, CH_4, O_2, Ar, and He) were determined by gas chromatography. The chemical compositions of fumarolic samples are reported in Table 1.

Heat flux involved in the diffuse degassing process

Heat flux through the soil in the study area was estimated from soil temperature measurements using the method of Dawson (1964) and described in Fridriksson et al. (2006). The temperature at 15 cm depth was measured at all points with a portable thermocouple. This method is based on correlation between soil temperature at 15 cm depth (t_{15}) and surface heat flux measured by a portable calorimeter. Where t_{15} was below 97 °C, the heat flux through the soil (q_s in watts per square meter) was estimated by:

$$q_s = 5.2 + 10^{-6} t_{15}^4 \quad (1)$$

where t_{15} is in degrees Celsius. If t_{15} was 97 °C or higher, the depth to the point where the soil temperature reaches that temperature (d_{97}; in centimeter) allows the estimation of the heat flow through soil by:

$$q_s = 10^{((\log d_{97} - 3.548)/-0.84)} \quad (2)$$

Regarding the heat flux involved in the diffuse degassing process, we followed the method proposed by Chiodini et al. (2001) and Frondini et al. (2004). This method uses CO_2 as a tracer of hydrothermal fluids, assuming that the H_2O/CO_2 ratio of hydrothermal fluids, before steam condensation, is recorded by fumarolic discharges. Chiodini et al. (2001) computed the heat flux, adding the following contributions: (a) The heat released by H_2O gas moving from the hydrothermal reservoir to the steam condensation zone; (b) the heat given off by CO_2 passing from the hydrothermal reservoir to atmospheric conditions; (c) the enthalpy of steam condensation at 100 °C, and (d) the heat lost by liquid water on cooling from 100 °C to the average seasonal value. He estimated that approximately 90 % of the total thermal energy at Solfatara volcano, Campi Flegrei was transported by H_2O and most of it is dissipated through steam condensation. Frondini et al. (2004) estimated the thermal energy release associated with condensation at Vesuvius volcano after adding the following two contributions: (a) the enthalpy of steam condensation at 100 °C and (2) the heat lost by liquid water on cooling from 100 °C to the average seasonal value.

Statistical and geostatistical treatment of the data

Probability plot technique (Tennant and White 1959; Sinclair 1974) was applied to the entire CO_2 efflux data sets to check whether the data represent one or more log-normal populations. The probability plot technique consists of plotting the logarithm of the data versus the cumulative frequency percent on a probability scale, arranged such that a normal (Gaussian) cumulative distribution plots as a straight

line. A bimodal distribution consisting of two log-normal populations plots as a curve. The inflection point of the curve allows us to distinguish the threshold value between both populations. Sequential Gaussian simulation (SGS), provided by the sgsim program (Deutsch and Journel 1998; Cardellini et al. 2003), was used for mapping and estimation of the diffuse CO_2 flux and heat flux. SGS was not applied to the H_2S data because of insufficient number of measurements where H_2S flux was detectable. To construct the spatial distribution map of H_2S efflux values and estimate the diffuse emission of this gas species, kriging was used as interpolation technique. SGS has been applied before in the study of soil diffuse degassing at volcanic and nonvolcanic systems (Cardellini et al. 2003; Frondini et al. 2004; Fridriksson et al. 2006; Padrón et al. 2007). The SGS procedure allows us to both interpolate the soil CO_2 efflux at nonsampled sites and assess the uncertainty of the total diffuse emission of carbon dioxide estimated for the entire studied area. The simulation is conditional and sequential, i.e., the variable is simulated at each unsampled location by random sampling of a Gaussian conditional cumulative distribution function (Cardellini et al. 2003).

Results

Soil diffuse CO_2 and H_2S degassing

Diffuse CO_2 and H_2S efflux values ranged from nondetectable to 17,666 and 722.3 $g m^{-2} day^{-1}$, respectively. A probability plot of CO_2 efflux values, using the methodology of Sinclair (1974), shows two distinct modes: normal I and normal II. These two distinct populations are known as background and peak, respectively. The graphical analysis (Fig. 2) shows two different populations for Hengill volcano, with a mean of 4.3 $g m^{-2} day^{-1}$ for the background population (normal I), which represented 79.6 % of the total data, and a mean of 1,091 $g m^{-2} day^{-1}$ for the peak population (normal II), which represented 9.6 % of the total data. Although the sampling distribution did not homogenously cover the studied area and the peak population is a disproportionally large fraction of the total data, the mean value of the peak population is unaffected. The background population can be attributed to biological activity and soil respiration by integrating most of the measured fluxes. Because the mean CO_2 efflux value of the peak population is two orders of magnitude higher than background values, we can assume that the peak population represents CO_2 diffuse degassing from the volcanic/hydrothermal system of Hengill.

The experimental variogram for CO_2 efflux SGS at Hengill was fitted with a spherical model with a nugget of 0.3, lag distance of 200 m, and range of 1,400 (Fig. 3a).

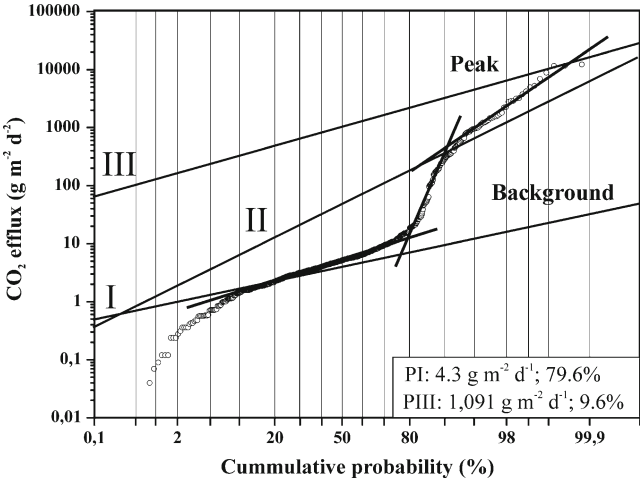

Fig. 2 Probability plot of the CO_2 efflux data measured at Hengill volcanic system. *Numerals I*, *II*, and *III* indicate the different log-normal modes separated. *Open circles* indicate the original data

Following the variogram model, 100 simulations were performed over a grid of 16,808 square cells (100×100 m), giving an area of 168.1 km^2. An average map (Fig. 3b) was constructed for each studied area using the average of the simulated values at each cell. To estimate the total diffuse CO_2 output released from the studied area to an uncertainty of 1 standard deviation, we considered the contribution of each cell obtained after SGS and averaged over 100 simulations. The average value for the total diffuse CO_2 released from the Hengill volcanic system and the standard deviation were 1,526 and 160 $t day^{-1}$, respectively. Because SGS was not used for H_2S efflux data, a rough estimate of the total diffuse H_2S output from the studied area was computed. Considering the volume bounded by the three-dimensional surface built up by the kriging in the contouring, it is estimated that about 8 $kg day^{-1}$ of diffuse H_2S is released by this volcanic system.

To quantify both the anomalous and the background CO_2 efflux from the studied area, we used the threshold value computed from the probability plot, 44.4 $g m^{-2} day^{-1}$. We assumed the contribution of the background population equals the sum of the interpolated cells between the minimum and the threshold CO_2 emission value. Likewise, the peak population contribution is the sum of the emission of the interpolated cells between the threshold and the maximum value. Following this assumption, background and peak population emissions are 1,073±105 and 453±43 t day^{-1}, respectively, where the uncertainty is equal to 1 standard deviation. As a result, endogenous volcanic/hydrothermal emission of CO_2 constitutes 29.7 % to the total diffuse CO_2 emission from the study area. To validate the estimated contribution of deep-seated CO_2 to the total CO_2 efflux, we delimited the main anomalous diffuse emission area at the NE flank of Hengill volcanic system (dotted line

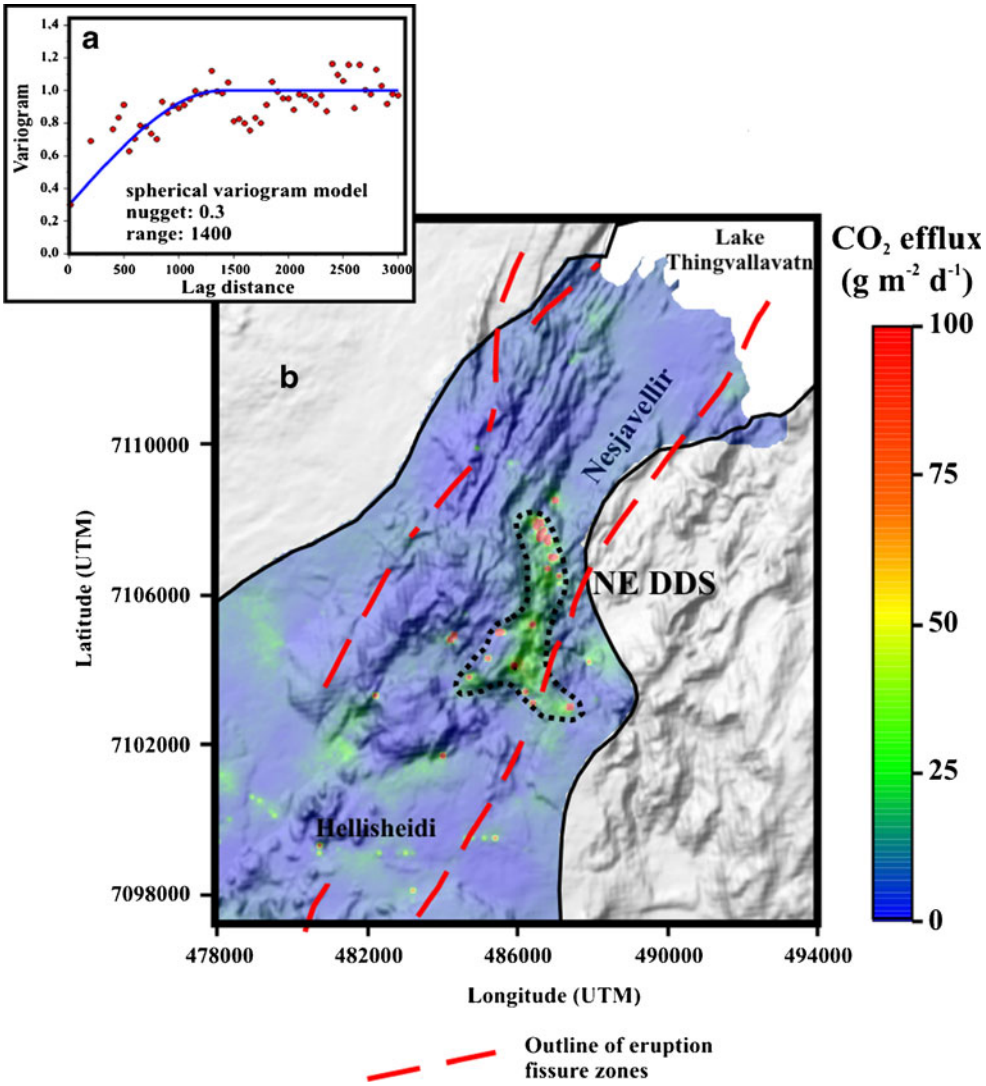

Fig. 3 **a** Omnidirectional experimental variogram of CO_2 efflux normal scores from the survey performed at Hengill volcanic system. *Solid blue line* represent the isotropic variogram model used in the simulation procedure. The parameters nugget and range refer to the variogram models. **b** Spatial distribution CO_2 efflux map obtained from a pointwise linear averaging of 100 SGS values for the Hengill volcanic system. *Dotted line* delimits the area selected at the NE side of Hengill to estimate the CO_2 emission from the most important anomalous area (pointwise linear averaging of 100 SGS values was also performed)

in Fig. 3b) and estimated the diffuse CO_2 emission from this area. The SGS was applied to the selected data and 100 simulations were performed over the NE diffuse degassing structure (DDS) using a grid of 30,445 squared cells (25× 25 m), resulting in an average diffuse CO_2 output of 602± 59 $t day^{-1}$. This value differs from the deep-seated CO_2 estimate of 453 $t day^{-1}$ that assumed the interpolated cells between the threshold and the maximum value from Sinclair's analysis can be explained by the contribution of background values in the SGS estimation.

Inspection of the soil CO_2 efflux distribution map (Fig. 3b) shows the existence of several areas of relatively high CO_2 efflux values (>100 $g m^{-2} day^{-1}$), most of them measured close to active thermal manifestations. The maximum CO_2 degassing rates were measured at the northeast flank of the Hengill central volcano close to the Nesjavellir power plant, suggesting a DDS with a SSW–NNE trend, coinciding with the main fissure zone, and indicating a structural control of the degassing process. At the study area, CO_2 escapes primarily in circular zones, suggesting a morphological control of the diffuse degassing phenomena. Owing to the bad accessibility at the upper part of the Hengill central volcano, it was only possible to carry out a few measurements in that area. Those measurements showed background CO_2 efflux values, though higher values might be present. At the south and southwest of Hengill central volcano, other alteration zones with increased emission rates were observed. However, at the western flank of Hengill, CO_2 efflux measured values were relatively low. Inspection of the H_2S efflux distribution map (Fig. 4) shows that generally H_2S efflux is very low or negligible in the study area due to the dissolution in the aquifer or oxidation in the soil environment. The maximum H_2S emission rate (722.3 $mg m^{-2} day^{-1}$) was also measured at the northeast flank of the Hengill central volcano, where anomalously high CO_2 efflux and soil temperatures were measured.

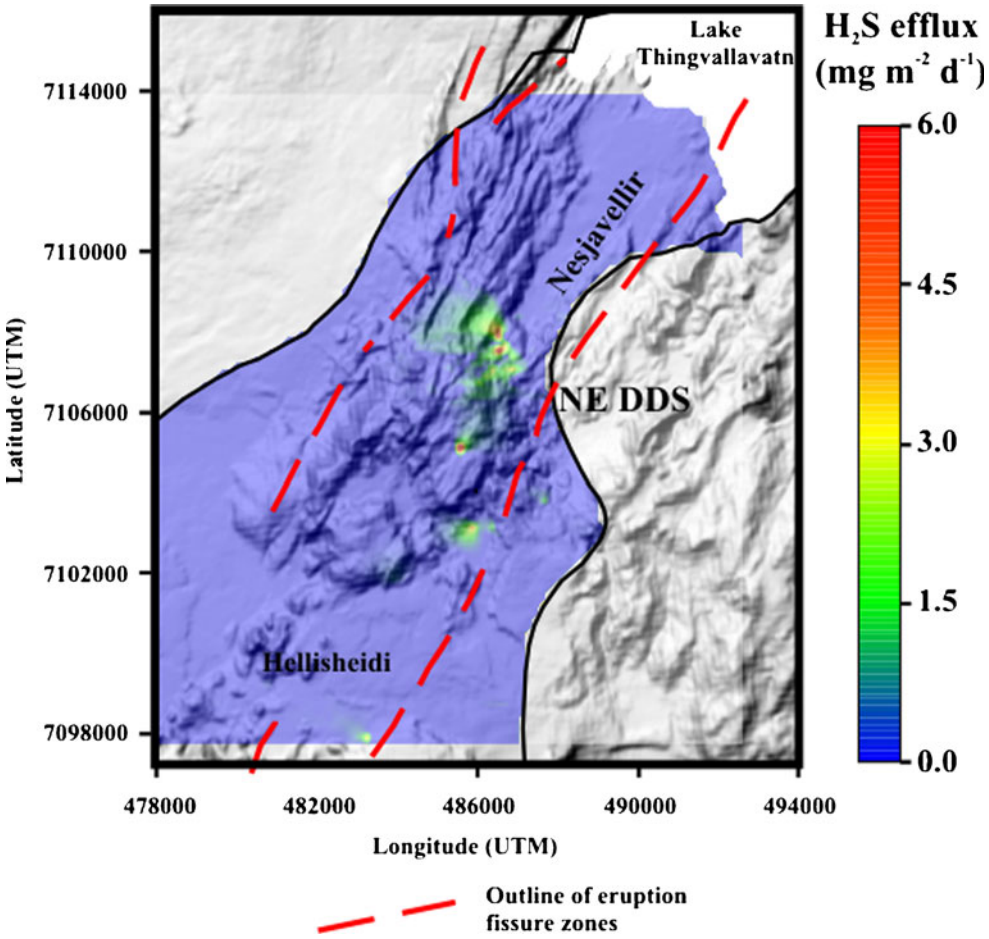

Fig. 4 Spatial distribution of soil H_2S efflux map constructed using the kriging method for the Hengill volcanic system

Soil temperatures and thermal energy release

Soil temperature values measured at 15 cm depth ranged from 1.4 to 100.2 °C, whereas estimated heat flux through soil ranged from zero to 2,464 W/m^2. The experimental variogram for soil temperature at Hengill was fitted with a spherical model with a nugget of 0.4 and range of 1,800 (Fig. 5a). Following the variogram model, 100 simulations were performed over a grid 16,808 squared cells (100×100 m). An average map (Fig. 5b) was constructed for each studied area using the average of the different values simulated at each cell. The measured maximum temperature was 100.2 °C close to the border to the Hromundartindur volcanic zone. In contrast, the determined minimum temperature was 5.9 °C on the upper part of the Hengill central volcano.

SGS was also used to evaluate the total heat flow from the surveyed area, following the same procedure as for the CO_2 efflux and temperature data. The experimental variogram for heat flux SGS at Hengill was also fitted with a spherical model with a nugget of 0.45 and a range of 2,000 (Fig. 6a). Following the variogram model, 100 simulations were performed over a grid 16,808 squared cells (100×100 m). A logmap of average heat flow was constructed for each studied area using the average of the different values simulated at each cell. The soil heat flow map shows a high-heat flow zone in the eastern region. Further to the southwest, in the area of the new Hellisheidi power plant, another high-heat flow zone is located. Compared to the eastern zone, temperatures and heat flow in the southwest zone reach lower values and the surface dimension is significantly smaller. The results of the 100 simulations are depicted in Fig. 6b, showing the mean heat flow of individual cells in the model. The average heat flow value of the 100 simulations over the study area was 11.5 MW.

To estimate the heat flow involved in the diffuse degassing process, CO_2 is used as a tracer of hydrothermal fluids (Chiodini et al. 2001; Fridriksson et al. 2006; Frondini et al. 2009), assuming that the H_2O/CO_2 ratio of hydrothermal fluids before steam condensation is recorded by fumarolic gases. All sampled fumarolic gases collected at the fumarolic fields (Skíðaskáli, Sleggjubeinsdalur, Þrymheimar, Innstidalur, Fremstidalur, Hveragerði, Reykjadalur, Ölkelduháls, Sandklettar, Köldulaugagil, and Nesjalaugagil) showed a similar temperature of 98–100 °C, the boiling temperature of water at Hengill altitude. Marty et al. (1991) addressed a unique source of hydrothermal fluids for the Hengill volcanic system and, even though the fumarolic gas composition shows differences in the most reactive gas species and in the H_2O and CO_2 contents, we have assumed as a representative H_2O/CO_2 ratio the average value of 88.6 by weight (Table 1). Because

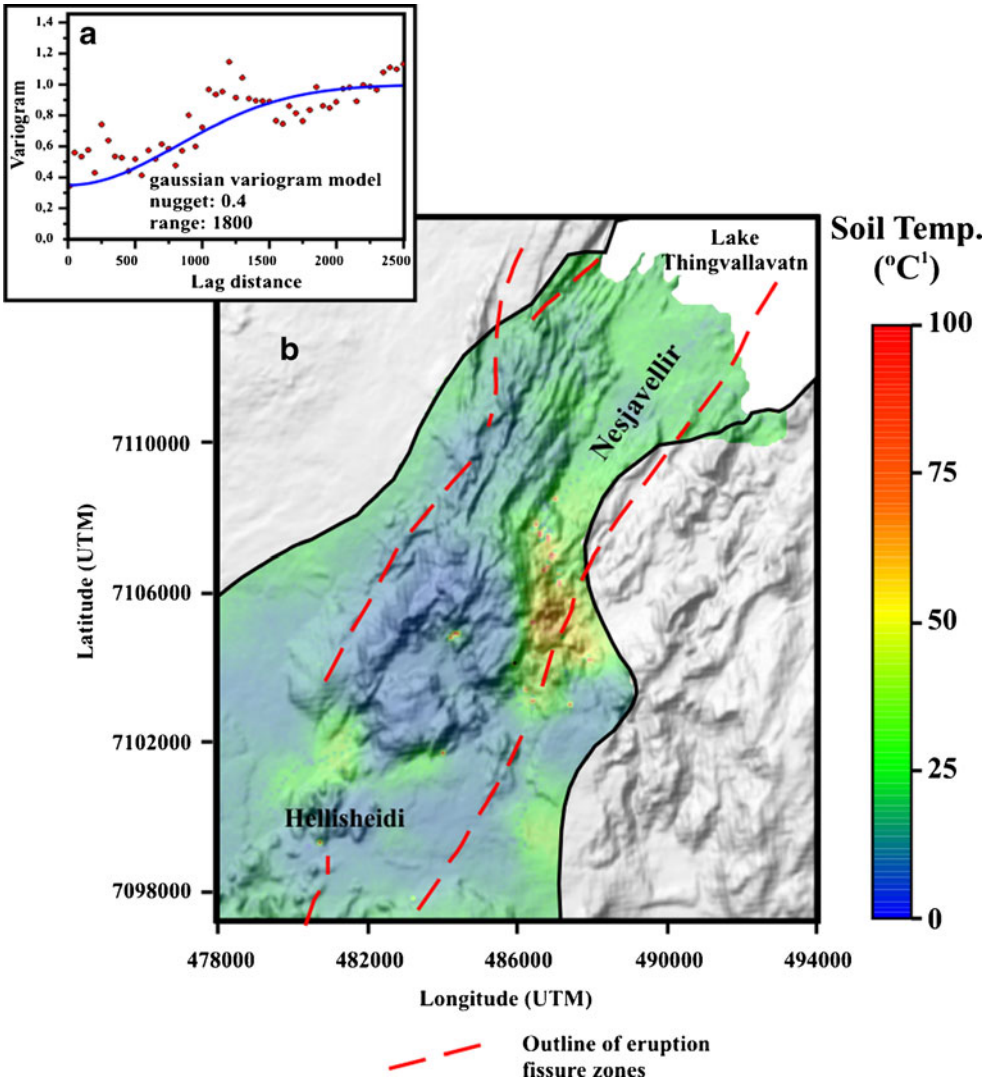

Fig. 5 **a** Omnidirectional experimental variogram of soil temperature normal scores from the survey performed at Hengill volcanic system. *Solid blue line* represent the isotropic variogram model used in the simulation procedure. The parameters nugget and range refer to the variogram models. **b** Spatial distribution of soil temperature map obtained from a pointwise linear averaging of 100 SGS values for the Hengill volcanic system

fumaroles at Hengill are low-temperature fumaroles, we can also assume that secondary processes (e.g., condensation) do not significantly affect the original ratios between H_2O, CO_2, and the unreactive gases (Chiodini et al. 2001). On the basis of this average ratio, we computed that 40,154 $tday^{-1}$ of steam are associated with the volcanic/hydrothermal CO_2 output of 453 $tday^{-1}$. However, if we take into account the range of H_2O/CO_2 ratios measured from the fumaroles (9.42–240.2), the minimum and maximum amount of steam would be 4,268 and 108,792 $tday^{-1}$, respectively.

By following the procedure described by Frondini et al. (2009), the thermal energy release associated with condensation of 40,154 $tday^{-1}$ of steam was calculated as 1.07×10^{14} J day^{-1}. This value was obtained by adding the following two contributions: (1) the enthalpy of steam condensation at 100 °C (4.66×10^{13} Jday^{-1}) given by the product of the total amount of steam condensed in 1 day (4.02×10^{10} g) times the enthalpy of evaporation at 100 °C (2,260 Jg^{-1}) (Keenan et al. 1969) and (2) the heat lost by liquid water on cooling from 100 °C to the average seasonal value of 10 °C (1.61×10^{13} Jday^{-1}), which is given by the product of the enthalpy lost by 1 g of water (ΔH=401.6 Jg^{-1}) times the mass of water (4.02×10^{10} g). The computed thermal energy of 1.07×10^{14} Jday^{-1} corresponds to a total heat flow of 1,237 MW, about 10 times higher than the 130 MW reported for the Reykjanes geothermal field in Iceland (Fridriksson et al. 2006). Using the same procedure, we also estimated the minimum and maximum thermal energy release associated with condensation of 4,268 and 108,792 $tday^{-1}$ of steam as 1.14×10^{13} and 2.89×10^{14} Jday^{-1}, respectively (131 and 3,351 MW).

Discussion and conclusions

Tectonic control of the diffuse degassing structure

The spatial distributions of diffuse CO_2 and H_2S efflux (Figs. 3b and 4b), soil temperature (Fig. 5b), and heat flow

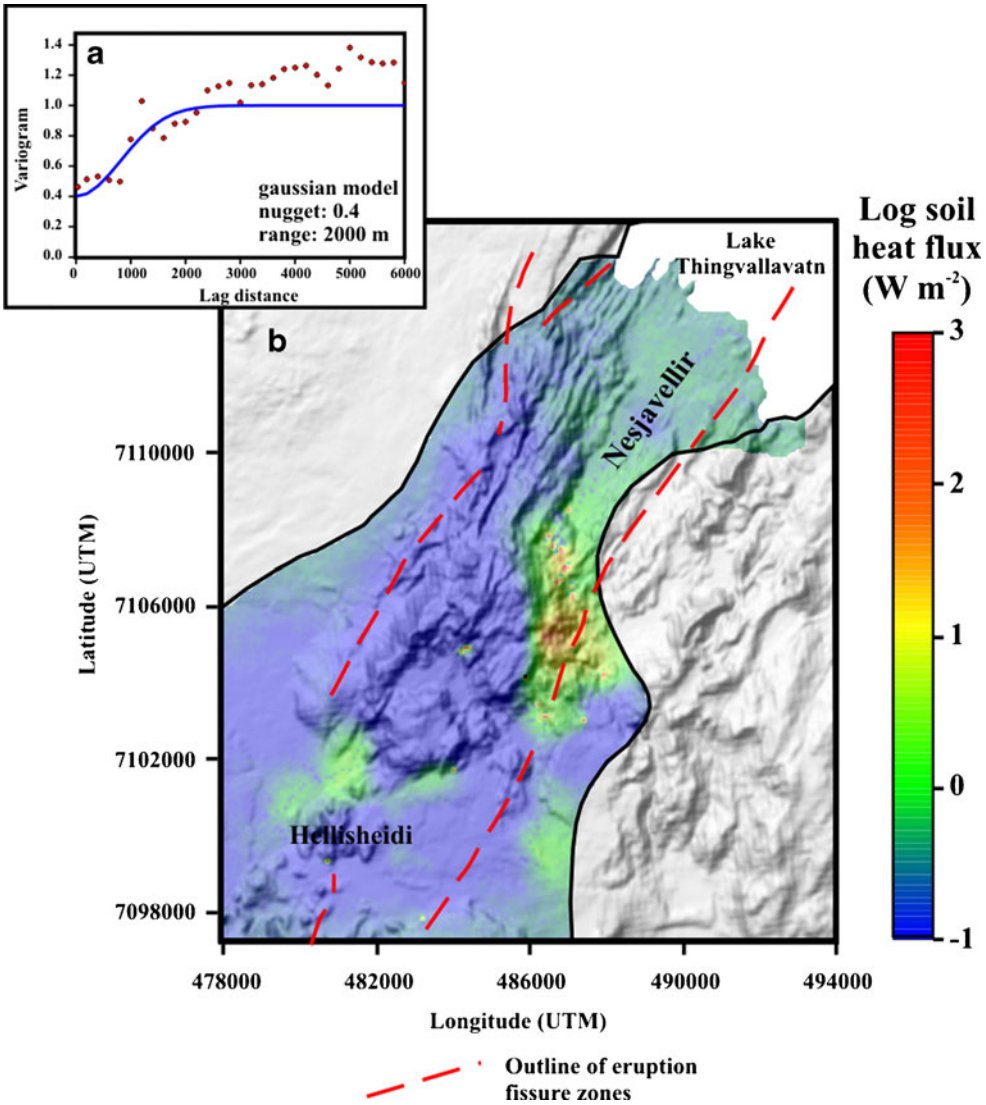

Fig. 6 **a** Omnidirectional experimental variogram of heat flux normal scores from the survey performed at Hengill volcanic system. *Solid blue line* represent the isotropic variogram model used in the simulation procedure. The parameters nugget and range refer to the variogram models. **b** Spatial distribution of heat flow map obtained from a pointwise linear averaging of 100 SGS values for the Hengill volcanic system

(Fig. 6b) in the studied area suggest a strong structural control of both CO_2 and H_2S diffuse emissions and heat loss, indicating well-defined NS lineation diffuse degassing and heat loss structures. Diffuse CO_2 efflux (Fig. 3b) and heat flow (Fig. 6b) anomalies were identified along a NS trend parallel to the NS lines inferred by the seismic activity that occurred between 1994 and 2000 (Árnason and Magnússon 2001; Björnsson et al. 2003). Diffuse H_2S efflux was not measurable throughout the entire study area and emission rates were very low, but the H_2S distribution (Fig. 4b) showed the same spatial pattern as diffuse CO_2 efflux and heat flux. These findings coincide with the V_P/V_S anomaly found by Jousset et al. (2011), which is elongated along the main hydrothermal features of the Hengill volcanic system (Fig. 1). Jousset et al. (2011) interpreted these earthquakes as resulting from stress changes within the geothermal reservoir, where hot fluid rises in the crust above the heat source. According to Árnason et al. (2010), much of this trend is correlated with a low-rigidity, low-permeability, relatively shallow clay cap, with thermal manifestations occurring at gaps in this cap connecting the thermal manifestations through the base of the clay cap to the immediately underlying reservoir. The surface geochemical and thermal anomalies identified during this study might be the surface evidence of the gaps from where deep fluids ascend to the surface.

Comparing the spatial distribution of diffuse CO_2 degassing and heat flow, we observe that at the north of the DDS, elevated heat flow through soil coincides with DDS. However, the south and the center parts of the DDS do not coincide as clearly with the most prominent heat flow anomaly. A complementary interpretation is that steam condensation beneath DDS is not homogeneous, being weaker at the south, where the main surface thermal anomaly occurs. Different CO_2 emission/soil temperature ratios have also been observed at other active volcanic–geothermal areas in Iceland (e.g., Reykjanes). Fridriksson et al. (2006) observed a different CO_2 emission/soil temperature ratio

along two well-defined linear diffuse degassing and heat loss structures. The authors addressed the observed differences as a result of different steam condensation rates under DDS.

The difference observed between heat flow through the surface at Hengill (11.5 MW) and the average thermal energy released by condensation of 40,154 $tday^{-1}$ of steam to the atmosphere (1,237 MW), associated with the volcanic/hydrothermal CO_2 output of 453 $tday^{-1}$, also supports the observed CO_2 emission/soil temperature ratios. The difference between these values is most probably a result of condensation of a large fraction of the steam in the subsurface, as hypothesized for Reykjanes, southwest Iceland (Fridriksson et al. 2006). Thermal energy from steam condensation at depth might be transported laterally out of the system by groundwater flow. This hypothesis is supported by TES resistivity and seismic data, which strongly support the existence of a seismically active fault zone located between the Hveragerdi (east of Hengill) and Hengill volcanic systems, acting as a fluid sink, probably due to lateral discharge towards the south (Björnsson et al. 2003).

Natural geothermal CO_2 emissions compared to emissions from power plants

The results of this study allow a comparison of the natural gas emissions from the Hengill central volcano to the emissions from the geothermal power plants Nesjavellir and Hellisheidi, both located in the study area. In 2010, the Nesjavellir power plant released 30,727 $tyear^{-1}$ of CO_2 and 13,340 $tyear^{-1}$ of H_2S into the atmosphere (Reykjavik Energy 2011), whereas the Hellisheidi power plant released 42,688 $tyear^{-1}$ of CO_2 and 9,384 $tyear^{-1}$ of H_2S. The installed capacity at Nesjavellir is 120 MW_e and 300 MW_t (Reykjavik Energy 2011), whereas at the Hellisheidi power plant, at the time of this study (phase 1), the installed capacity was 90 MW_e, although this was increased to a production capacity of 303 MW_e and 133 MW_t by 2011 (http://www.or.is/English/Projects/HellisheidiGeothermalPlant/).

The volcanic/hydrothermal CO_2 output of the Hengill volcanic system of 453 $tday^{-1}$ amounts to an annual CO_2 output of 165,345 $tyear^{-1}$. The total CO_2 emission from the Reykjavik Energy power plants in the area amounts to 73,415 $tyear^{-1}$ or slightly less than half of the natural emission in 2006. A similar ratio is observed at the Krafla geothermal field in NE Iceland where the natural emission of CO_2 of geothermal origin through diffuse degassing amounts to 84,000 $tyear^{-1}$ (Ármannsson et al. 2007). This compares to annual CO_2 emission from the 60 MW_e Krafla power plant, which has emissions between 40,000 and 44,000 $tyear^{-1}$ in the last 5 years (Landsvirkjun 2012). The ratio between anthropogenic and natural CO_2 emissions from the Hengill system is more or less the same as that for the Krafla system, i.e., natural emissions amount to slightly more than twice the amount released from the power plants.

The ratio of anthropogenic to natural gas emissions from the Reykjanes system is different from that from the Hengill and Krafla areas. Fridriksson et al. (2006) reported observed CO_2 emissions from the geothermal field of about 5,100 t $year^{-1}$ and they estimated the emissions from the 100-MW_e power plant that was under construction at the time at 31,000 $tyear^{-1}$. After the commissioning of the power plant, the geothermal surface activity increased significantly (Fridriksson et al. 2010), and in 2010, the annual natural emission of CO_2 via diffuse degassing at Reykjanes amounted to 12,660 $tyear^{-1}$ (Óladóttir and Snæbjörnsdóttir 2011), while the CO_2 emission from the Reykjanes power plant amounted to 26,940 $tyear^{-1}$ (Óskarsson and Fridriksson 2011). Thus, while the ratio of power plant emissions to diffuse degassing in Hengill and Krafla are both approximately 1:2, the ratio for Reykjanes is closer to 2:1.

The estimated CO_2 output of 453 $tday^{-1}$ is in the same order of magnitude as estimations reported for other active volcanic areas (Brombach et al. 2001; Chiodini et al. 1996, 2001, 2007; Frondini et al. 2004; Hernández et al. 2001a, 2003; Notsu et al. 2005; Pérez et al. 2004; Salazar et al. 2001). However, it should be noted that this is an underestimation of the total CO_2 discharge from the Hengill volcanic system because CO_2 dissolved by groundwater and CO_2 discharged through fumaroles and steam-heated mud pools have not been considered in this study. The absence of extensive surface manifestations in large parts of the productive geothermal reservoirs in the Hengill system, e.g., around the Hellisheidi power plant, suggests that considerable amounts of CO_2 from the reservoir may be dissolved in groundwater before it reaches the surface. On the other hand, the experience from Reykjanes (Fridriksson et al. 2006, 2010) suggests that emissions through steam vents and steam-heated mud pools are probably not as significant as diffuse degassing. In 2004, diffuse degassing constituted 97.5 % of the total natural emission, while steam vents and mud pits emitted the remaining 2.5 % (Fridriksson et al. 2006). In 2007, after the commissioning of the power plant had invigorated the surface activity at Reykjanes, diffuse degassing still constituted 90 % of the total natural CO_2 emission from the field, whereas emission from steam vents and pits amounted to 10 % of the total (Fridriksson et al. 2010).

Diffuse degassing surveys at regular intervals over a period of several years will be an important geochemical tool to understand the system's behavior, especially concerning the consistency of emission rates and propagation or retreat of fumarolic areas. Such periodic studies are important to evaluate the effect of geothermal production on the surface activity, as has been done in Reykjanes

(Fridriksson et al. 2010). Further, these studies also provide important baseline information to interpret signs on future magmatic events in the Hengill volcanic system. Future investigations should consider gas dissolving in groundwater or streams, which can imperceptibly discharge gas from the volcanic system.

Soil diffuse H_2S emissions

As noted above, the H_2S flux through the surface was below the detection limit in the majority of the measurement points. Nevertheless, the total H_2S emission was estimated to be 8 $kg\,day^{-1}$. This value is miniscule compared to the geothermal CO_2 flux of 453 $t\,day^{-1}$. The CO_2/H_2S mass ratio in the gas emitted from Hellisheidi and Nesjavellir power plants is 4.5 and 2.3, respectively. This mass ratio for the fumarole steam samples shown in Table 1 ranges from 6.1 to 157, but most samples have a CO_2/H_2S mass ratio between 10 and 30. The CO_2/H_2S mass ratio for the geothermal gas emitted through the soil in the Hengill area is 56,600, which is more than four orders of magnitude higher than that for the gas emitted from the power plants and more than three orders of magnitude higher than that for the fumarole steam. This suggests that H_2S is removed in large quantity from the geothermal gas in the soil environment, which is consistent with the fact that this gas is thermodynamically unstable in the presence of O_2. If we assume that the CO_2/H_2S mass ratio in the geothermal gas ascending from the geothermal reservoirs in Hengill is between 10 and 30, then the mass of H_2S that is removed annually from the geothermal gas in the soil environment is 45.3 to 15.1 $t\,year^{-1}$.

Acknowledgments This research was financially supported by a grant from the Spanish Ministry of Science and Technology (CGL2005-07509) as well as by the Cabildo Insular de Tenerife (Spain). Field and logistic support was also provided by ISOR and Reykjavik Energy. The authors thank one anonymous reviewer and Williams C. Evans for their constructive comments.

References

Allard P, Carbonelle J, Dajlevic D, Le Bronec J, Morel P, Robe MC, Maurenas JM, Faivre-Pierret R, Martins D, Sabroux JC, Zettwoog P (1991) Eruptive and diffuse emissions of CO_2 from Mount Etna. Nature 351:387–391

Ármannsson H, Fridriksson T, Wiese F, Hernández P, Pérez N (2007) CO_2 budget of the Krafla geothermal system, NE-Iceland. In: Bullen TD, Wang Y (eds) Water–rock interaction. Taylor & Francis Group, London, pp 189–192

Árnason K, Magnússon I (2001) Geothermal activity in the Hengill area. Results from resistivity mapping. Orkusfnun Report, in Icelandic with English abstract OS.2001/091, p 250

Árnason K, Eysteinsson H, Hersir G (2010) Joint 1D inversion of TEM and MT data and 3D inversion of MT data in the Hengill area, SW Iceland. Geothermics 39:13–34

Arnórsson S, Gunnlaugsson E (1985) New gas geothermometers for geothermal exploration. Calibration and application. Geochim Cosmochim Acta 49:1307–1326

Arnórsson S, Bjarnaso JÖ, Giroud N, Gunnarsson I, Stefánsson A (2006) Sampling and analysis of geothermal fluids. Geofluids 6 (3):203–216

Baubron JC, Allard P, Toutain JP (1990) Diffuse volcanic emissions of carbon dioxide from Vulcano Island, (Italy). Nature 344:51–53

Björnsson A, Hersir GP, Björnsson G (1986) The Hengill high-temperature area in SW-Iceland. Reg Geophys Surv Geotherm Resour Counc Trans 10:205–210

Björnsson G, Hjartarson A, Bödvarsson GS, Steingrímsson, B (2003) Development of a 3-D geothermal reservoir model for the greater Hengill volcano in SW-Iceland. Proceedings of the Tough Symposium, Lawrence Berkeley National Laboratory, Berkeley, California, 12–14 May

Bodvarsson GS, Bjornsson S, Gunnarsson A, Gunnlaugsson E, Sigurdsson O, Stefansson V, Steingrimsson B (1990) The Nesjavellir geothermal field, Iceland. Part 1. Field characteristics and development, of a three-dimensional numerical model. Geotherm Sci & Tech 2(3):189–228

Brombach T, Hunziker C, Chiodini G, Cardellini C, Marini L (2001) Soil diffuse degassing and thermal energy fluxes from the southern Lakki plain, Nysiros (Greece). Geophys Res Lett 28(1):69–72

Carapezza ML, Inguaggiato S, Brusca L, Longo M (2004) Geochemical precursors of the activity of an open-conduit volcano: the Stromboli 2002–2003 eruptive events. Geophys Res Lett 31: L07620. doi:10.1029/2004GL019614

Carapezza ML, Barberi F, Ranaldi M, Ricci T, Tarchini L, Barrancos J, Fischer C, Perez N, Weber K, Di Piazza A, Gattuso A (2011) Diffuse CO_2 soil degassing and CO_2 and H_2S concentrations in air and related hazards at Vulcano Island (Aeolian arc, Italy). J Volcanol Geotherm Res. doi:10.1016/j.jvolgeores.2011.06.010

Cardellini G, Chiodini G, Frondini F (2003) Application of stochastic simulation to CO_2 flux from soil: mapping and quantification of gas release. J Geophys Res 108(B9):2425. doi:10.1029/2002JB002165

Chiodini G, Frondini F, Raco B (1996) Diffuse emission of CO_2 from the Fossa crater Vulcano Island (Italy). Bull Volcanol 58:41–50

Chiodini G, Cioni R, Guidi M, Raco B, Marini L (1998) Soil CO_2 flux measurements in volcanic and geothermal areas. Appl Geochem 13:543–552

Chiodini G, Frondini F, Cardellini C, Granieri D, Marini L, Ventura G (2001) CO_2 degassing and energy release at Solfatara volcano, Campi Flegrei, Italy. J Geophys Res 106(B8):16213–16221

Chiodini G, Baldini A, Barberi F, Carapezza ML, Cardellini C, Frondini F, Granier D, Ranaldi M (2007) Carbon dioxide degassing at Latera caldera (Italy): evidence of geothermal reservoir and evaluation of its potential energy. J Geophys Res 112:B12204. doi:10.1029/2006JB004896

Dawson GB (1964) The nature and assessment of heat flow from hydrothermal areas. N Z J Geol Geophys 7:155–171

Deutsch CV, Journel AG (1998) GSLIB: Geostatistical Software Library and user's guide. Oxford University Press, New York, p 369

Foulger GR (1988) The Hengill triple junction, SW Iceland. 1. Tectonic structure and the spatial and temporal distribution of local earthquakes. J Geophys Res 93(B11):493–506

Foulger GR (1995) The Hengill geothermal area, Iceland: variation of temperature gradients deduced from the maximum depth of seismogenesis. J Volcanol Geotherm Res 65:119–133

Foulger GR, Arnott SA (1993) Local tomography: volcanoes and the accretionary plate boundary in Iceland. In: Iyer HM, Hirahara K

(eds) Seismic tomography: theory and practise. Chapman and Hall, London, pp 644–675

Foulger GR, Toomey DR (1989) Structure and evolution of the Hengill-Grensdalur central volcano complex, Iceland: geology, geophysics and seismic tomography. J Geophys Res 94:17511–17522

Franzson H, Kristjánsson BR, Gunnarsson G, Björnsson G, Hjartarson A, Steingrímsson B, Gunnlaugsson E, Gíslason G (2005) The Hengill-Hellisheiði geothermal field. Development of a conceptual geothermal model. Proceedings of the World Geothermal Congress 2005, Antalya, Turkey, 24–29 April

Fridriksson T, Kristjánsson BR, Ármannsson H, Margrétardóttir E, Ólafsdóttir S, Chiodini G (2006) CO_2 emissions and heat flow through soil, fumaroles, and steam heated mud pools at the Reykjanes geothermal area, SW Iceland. Appl Geochem 21 (9):1551–1569

Fridriksson T, Óladóttir AA, Jónsson P, Eyjólfsdóttir EI (2010) The response of the Reykjanes geothermal system to 100 MW_e power production: fluid chemistry and surface activity. Proceedings of the World Geothermal Congress 2010, Bali Indonesia. Available at http://www.geothermal-energy.org/pdf/IGAstandard/WGC/2010/0626.pdf

Friese N, Krumbholz M, Burchardt S, Gudmundsson A (2005) Tectonics of the Hengill volcano, Southwest Iceland. Abstract V21D-0638, Am Geophys Union, Fall Meeting 2005

Frondini F, Chiodini G, Caliro S, Cardellini C, Granieri D, Ventura G (2004) Diffuse CO_2 degassing at Vesuvio, Italy. Bull Volcanol 66:642–651

Frondini F, Caliro S, Cardellini C, Chiodini G, Morgantini N (2009) Carbon dioxide degassing and thermal energy release in the Monte Amiata volcanic–geothermal area (Italy). Appl Geochem 24(5):860–875. doi:10.1016/japgeochem200901010

Gerlach TM, Graeber EJ (1985) Volatile budget of Kilauea volcano. Nature 313(no 6000):273–277

Gerlach TM, Doukas MP, McGee KA, Kessler R (2001) Soil flux and total emission rates of magmatic CO_2 at the Horeshoe Lake tree kill, Mammoth Mountain, California, 1995–1999. Chem Geol 177:101–116

Giggenbach WF (1980) Geothermal gas equilibria. Geochim Cosmochim Acta 44:2021–2032

Granieri D, Carapezza ML, Chiodini G, Avino R, Caliro S, Ranaldi M, Ricci T, Tarchini L (2006) Correlated increase in CO_2 fumarolic content and diffuse emission from La Fossa crater (Vulcano, Italy): evidence of volcanic unrest or increasing gas release from a stationary deep magma body? Geophys Res Lett 33:L13316. doi:10.1029/2006GL026460

Hernández PA, Pérez NM, Salazar JM, Nakai S, Notsu K, Wakita H (1998) Diffuse emissions of carbon dioxide, methane, and hellium-3 from Teide volcano, Tenerife, Canary Islands. Geophys Res Lett 25:3311–3314

Hernández PA, Notsu K, Salazar JM, Mori T, Natale G, Okada H, Virgili G, Shimoike Y, Sato M, Pérez NM (2001a) Carbon dioxide degassing by advective flow from Usu volcano, Japan. Science 292:83–86

Hernández PA, Salazar JM, Shimoike Y, Mori T, Notsu K, Perez NM (2001b) Diffuse emission of CO_2 from Miyakejima volcano, Japan. Chem Geol 177:175–185

Hernández PA, Notsu K, Tsurumi M, Mori T, Ohno M, Shimoike Y, Salazar JM, Pérez, NM (2003) Carbon dioxide emissions from soils at Hakkoda, North Japan. J Geophys Res 108:6-1–6-10

Hernández PA, Notsu K, Okada H, Mori T, Sato M, Barahona F, Pérez NM (2006) Diffuse emission of CO_2 from Showa-Shinzan, Hokkaido, Japan: a sign of volcanic dome degassing. Pure Appl Geophys 163:869–881

Ingólfsson Ó, Sigmarsson O, Sigmundsson F, Símonarson L (2008) The dynamic geology of Iceland. Jökull 58:1–2

Jousset P, Haberland C, Bauer K, Arnason K (2011) Hengill geothermal volcanic complex (Iceland) characterized by integrated geophysical observations. Geothermics 40(1):1–24

Keenan JH, Keyes FG, Hill PG, Moore JG (1969) Steam tables—thermodynamic properties of water including vapor, liquid and solid phases (international edition metric units). Wiley, New York, p 162

Landsvirkjun (2012) Landsvirkjun annual report 2011. Landsvirkjun, Reykjavík, Iceland, pp 108. Available at http://www.landsvirkjun.is/um-landsvirkjun/utgefid-efni/arsskyrsla

Lewicki L, Hilley GE, Tosha T, Aoyagi R, Yamamoto K, Benson SM (2007) Dynamic coupling of volcanic CO_2 flow and wind at the Horseshoe Lake tree kill, Mammoth Mountain, California. Geophys Res Lett 34:L03401. doi:10.1029/2006gl028848

Marty B, Gunnlaugsson E, Jambon A, Óskarsson N, Ozima M, Pineau F, Torssander P (1991) Gas geochemistry of geothermal fluids, the Hengill area, southwest rift zone of Iceland. Chem Geol 91:207–225

Notsu K, Sugiyama K, Hosoe M, Uemura A, Shimoike Y, Tsunomori F, Sumino H, Yamamoto J, Mori T, Hernández PA (2005) Diffuse CO_2 efflux from Iwojima volcano, Izu-Ogasawara arc, Japan. J Volcanol Geotherm Res 139:147–161

Óladóttir AÓ, Snæbjörnsdóttir SÓ (2011) Observations on surface activity in the Reykjanes geothermal field. ÍSOR Report 2011/055, Iceland GeoSurvey, Reykjavik, p 29

Óskarsson F, Fridriksson T (2011) Reykjanes production field. Geochemical monitoring in 2010. ÍSOR Report 2011/050, Iceland GeoSurvey, Reykjavík, p 51

Padrón E, Melián G, Nolasco D, Barrancos J, Hernández PA, Pérez N (2007) Precursory diffuse carbon dioxide degassing related to seismic activity in El Hierro islands, Canary Islands, Spain. Pure Appl Geophys 165:95–114

Padrón E, Hernández PA, Toulkeridis T, Pérez NM, Marrero R, Melián G, Virgili G, Notsu K (2008) Diffuse CO_2 emission rate from Pululahua and the lake-filled Cuicocha calderas, Ecuador. J Volcanol Geotherm Res 176(1):163–169

Parkinson KJ (1981) An improved method for measuring soil respiration in the field. J Appl Ecol 18:221–228

Pérez NM, Salazar JML, Hernández PA, Soriano T, Lopez K, Notsu K (2004) Diffuse CO_2 and ^{222}Rn degassing from San Salvador volcano, El Salvador, Central America. Bull Geol Soc Am 375:227–236

Pérez NM, Hernández PA, Padrón E, Cartagena R, Olmos R, Barahona F, Melián G, Salazar P, López DL (2006) Anomalous diffuse CO_2 emission prior to the January 2002 short-term unrest at San Miguel Volcano, El Salvador, Central America. Pure Appl Geophys 4:883–896. doi:10.1007/s00024-006-0050-1

Pérez N, Hernández PA, Barrancos J, Melian G, Henriquez B, Mora R, Toulkeridis T (2007) H_2S emission from Santa Ana (El Salvador), Masaya (Nicaragua) and Poas (Costa Rica) and Sierra Negra (Galpagos) volcanoes. Proceedings of the IUGG XXIV General Assembly, 2–13 July, Perugia, Italy, VS015, Oral Presentation 6906

Reykjavík Energy (2011) Reykjavik energy annual report 2010. Reykjavik Energy, Reykjavik, p 50

Rogie JD, Kerrick DM, Sorey ML, Chiodini G, Galloway DL (2001) Dynamics of carbon dioxide emission at Mammoth Mountain, California. Earth Planet Sci Lett 188:535–541

Sæmundsson K (2006) The 1789 rifting event in the Hengill volcanic system, SW-Iceland. Am Geophys Union, Fall Meeting, Abstract T41B-1568

Salazar JML, Hernández PA, Pérez NM, Melián G, Álvarez J, Segura F, Notsu K (2001) Diffuse emissions of carbon dioxide from Cerro Negro volcano, Nicaragua, Central America. Geophys Res Lett 28:4275–4278

Salazar JML, Hernández PA, Pérez NM, Olmos R, Barahona F, Cartagena R, Soriano T, Lopez K, Notsu K (2004) Spatial and temporal variations of diffuse CO_2 degassing at Santa Ana–Izalco–Coatepeque volcanic complex, El Salvador, Central America. Bull Geol Soc Am Spec Pap 375:135–146

Salazar P, Pereda E, Padron E, Melian G, Perez NM, Hernández PA (2005) Secular variations of soil H_2S efflux at Teide volcano, Tenerife, Canary Islands. Geophys Res Abstr 7:10096

Sinclair AJ (1974) Selection of thresholds in geochemical data using probability graphs. J Geochem Explor 3:129–149

Tennant CB, White ML (1959) Study of the distribution of some geochemical data. Econ Geol 54:1281–1290

Toutain JP, Baubron JC, Le Broned J, Allard P, Briole P, Marty B, Miele G, Tedesco D, Luongo G (1992) Continuous monitoring of distal gas emanations at Vulcano, southern Italy. Bull Volcanol 54:147–155

Tryggvason A, Rögnvaldsson ST, Flóvenz ÓG (2002) Three-dimensional imaging of the P- and S-wave velocity structure and earthquake locations beneath Southwest Iceland. Geophys J Int 151(3):848–866

Vogfjörd KS, Hjaltadóttir S, Slunga R (2005) Volcano-tectonic Interaction in the Hengill Region, Iceland during 1993–1998. Eur Geosci Union Geophys Res Abst 7:09947

Voltaggio M, Spadoni M (2009) Mapping of H_2S fluxes from the ground using copper passive samplers: an application study at the Zolforata di Pomezia degassing area (Alban Hills, Central Italy). J Volcanol Geotherm Res 179:56–68